NOAA Technical Memorandum OAR ETL-298

A CASE STUDY OF THE IMPACT OF OFF-SHORE P-3 OBSERVATIONS ON THE PREDICTION OF COASTAL WIND AND PRECIPITATION

J-W. Bao
Environmental Technology Laboratory

S.A. Michelson
CIRES, Environmental Technology Laboratory
and The University of Colorado at Boulder

J.M. Wilczak
F.M. Ralph
Environmental Technology Laboratory

P.O.G. Persson
CIRES, Environmental Technology Laboratory
and The University of Colorado at Boulder

R.J. Zamora
Environmental Technology Laboratory

Environmental Technology Laboratory
Boulder, Colorado
March 2000

noaa NATIONAL OCEANIC AND ATMOSPHERIC ADMINISTRATION / Oceanic and Atmospheric Research Laboratories

NOAA Technical Memorandum OAR ETL-298

A CASE STUDY OF THE IMPACT OF OFF-SHORE P-3 OBSERVATIONS ON THE PREDICTION OF COASTAL WIND AND PRECIPITATION

J-W. Bao
Environmental Technology Laboratory

S.A. Michelson
CIRES, Environmental Technology Laboratory
and The University of Colorado at Boulder

J.M. Wilczak
F.M. Ralph
Environmental Technology Laboratory

P.O.G. Persson
CIRES, Environmental Technology Laboratory
and The University of Colorado at Boulder

R.J. Zamora
Environmental Technology Laboratory

Environmental Technology Laboratory
Boulder, Colorado
March 2000

UNITED STATES DEPARTMENT OF COMMERCE

William M. Daley
Secretary

NATIONAL OCEANIC AND ATMOSPHERIC ADMINISTRATION

D. JAMES BAKER
Under Secretary for Oceans and Atmosphere/Administrator

Oceanic and Atmospheric Research Laboratories

David L. Evans
Director

NOTICE

Mention of a commercial company or product does not constitute an endorsement by the NOAA Oceanic and Atmospheric Research Laboratories. Use of information from this publication concerning proprietary products or the test of such products for publicity or advertising purposes is not authorized.

For sale by the National Technical Information Service, 5285 Port Royal Road
Springfield, VA 22061

CONTENTS

A CASE STUDY OF THE IMPACT OF OFF-SHORE P-3 OBSERVATIONS ON THE PREDICTION OF COASTAL WIND AND PRECIPITATION

J-W. Bao,[1] S.A. Michelson,[2] J.M. Wilczak,[1] F.M. Ralph,[1] P.O.G Persson,[2] and R.J. Zamora[1]

[1]NOAA/Environmental Technology Laboratory, Boulder, CO

[2]CIRES, University of Colorado and NOAA/Environmental Technology Laboratory, Boulder, CO

March 1, 2000

ABSTRACT

This report summarizes a case study in which numerical experiments are carried out to assess the impact of CALJET P-3 aircraft data on the forecast of winds and precipitation over the California coast. The case chosen for this study is the storm that made landfall along the California coast between 1200 UTC 2 February and 0000 UTC 4 February 1998. In the experiments, the "nudging method" is used for assimilation of dropsonde data (between the surface and 500 mb) and flight-level soundings (between 1000 and 850 mb). The assimilation significantly changes the low-level winds in the model 6 h into the simulation, but the movement of the cyclone, which is different from observations, is not altered. The major finding from the experiments is that the P-3 data has a minimal impact on the 12-24 h coastal wind and precipitation forecasts. This is reflected by the fact that the threat and bias scores for hourly model forecasted precipitation are changed only slightly by assimilation of the data. One possible explanation for the minimal data impact is that in this case, the errors in the coastal wind and precipitation forecasts are mainly due to errors in the position of the cyclone and front; the P-3 data are not sufficient to correct them. Adjoint sensitivity analyses provide insight into why the impact of the in situ data is minimal. The sensitivity results indicate that the P-3 observations were not taken in the area where the model forecasted evolution of the surface wind associated with the low-level jet is most sensitive to the perturbations of the model state. Further trajectory analyses support this explanation.

A CASE STUDY OF THE IMPACT OF OFFSHORE P-3 OBSERVATIONS ON THE PREDICTION OF COASTAL WIND AND PRECIPITATION

J-W. Bao,[1] S.A. Michelson,[2] J.M. Wilczak,[1] F.M. Ralph,[1] P.O.G Persson,[2] and R.J. Zamora[1]

[1]NOAA/Environmental Technology Laboratory, Boulder, CO
[2]CIRES, University of Colorado and NOAA/Environmental Technology Laboratory, Boulder, CO

1. INTRODUCTION

One of the goals of the California Land Falling Jets Experiment (CALJET) conducted in 1998 was to provide the research community with in situ offshore observations of the mesoscale structure of the low-level jet (LLJ) within the warm sector of landfalling cyclones (Ralph et al. 1999). In situ data sets are regarded as valuable to the investigation of whether additional special observations made off-shore have an impact on short-range forecasts of hazardous weather events on the California coast. It has been hypothesized that because the predictability of damaging wind and heavy rainfall on this coast is related to the predictability of the mesoscale structure of the LLJ , additional observations of the LLJ offshore will lead to improvement in the predictability of downstream coastal wind and precipitation caused by the interaction of the LLJ with coastal topography. The purpose of the case study reported here is to test this hypothesis, using the CALJET in situ observations taken during one of the deployments of the National Oceanographic and Atmospheric Administration's (NOAA's) P-3 aircraft.

The P-3 in situ data sets include dropsonde and flight-level data. The former contain soundings of temperature, moisture, and wind from the dropping level (typically at about 500 mb) to the surface. The latter provide additional soundings of temperature and wind that were derived from P-3 ascents and descents. Although observations of a broad area of the troposphere upstream have proven to be crucial for short-range forecasts downstream, it is not known how much impact in situ observations taken upstream in a small area of the lower troposphere have on short-range forecasts downstream. This study is expected to shed new light on this subject.

The predictability of mesoscale features of the LLJ in the warm sector of landfalling cyclone systems is limited by errors in both model physics and the initial state. Since a cyclone is a synergetic

system, involving motions on different temporal and spatial scales, any forecasting errors in a numerical model of the mesoscale features of the LLJ may be influenced by forecast errors in other components of the cyclone. The degree of such influence may vary from case to case and may also be dependent on the model physics. It is therefore important to test the aforementioned hypothesis under different weather scenarios, model resolutions, and choices of model physics. Evaluation of such varying impacts will be especially beneficial to mesoscale weather forecasting in areas where upstream observations are sparse, because in these areas forecasting often must rely on numerical forecast models.

This report presents a case study in which numerical experiments are carried out first to investigate to what degree additional in situ observations of the LLJ can affect downstream forecasts of wind and precipitation in a landfalling storm event, and then to see how much this effect depends on the choice of convective parameterization schemes and model resolutions. Then, a sensitivity analysis is performed using the adjoint method to obtain insight into the impact of the in situ data revealed by the numerical experiments. Finally, a trajectory analysis is performed using the numerical model output to seek physical explanations for the data impact. A brief description of the case used in the study will be provided in section 2 of this report. Aspects of numerical experiments will be described in section 3. Numerical results of data impact will be presented in section 4. Results of sensitivity analyses using the adjoint and trajectory methods will be described in section 5, followed by a discussion and summary in section 6.

2. OVERVIEW OF THE STORM

To investigate the impact of in situ observations taken during CALJET on the prediction of coastal wind and precipitation, numerical simulations are carried out for the storm that made landfall along the California coast between 1200 UTC 2 February and 0000 UTC 4 February 1998. The event involved two stages. The first was the northward advance of a warm front, which caused up to 177 mm (7.0 in) of rain in the mountains north of Santa Barbara in 24 h, ending at 1800 UTC 2 February. The second stage was the landfalling of the LLJ and cold front southeast of the cyclone center on 3

February. In the second stage, the prefrontal LLJ brought significant winds and flooding to the coastal regions of California. The interaction of the LLJ with the terrain was regarded as a major factor in the severe weather that followed, including the 314 mm (12.4 in) of rain that fell in the 24 h period from 1800 UTC 2 February to 1800 UTC 3 February in the coastal mountains south of Monterey.

3. NUMERICAL EXPERIMENTS

a. Model configuration

The numerical model used in this study is the nonhydrostatic version of the Pennsylvania State University/National Center for Atmospheric Research (NCAR) mesoscale modeling system (MM5) (Grell et al., 1994). Two sets of nested grids are used. The first set (G1) is doubly nested: 36 km resolution grid (121 by 121 grid points) covering most of the western United States and a large portion of the eastern Pacific Ocean; and a 12 km grid (166 by 166 grid points) covering California, Oregon, and the Pacific Ocean out to about 140°W (fig. 1a). A total of 25 σ layers are used, with the lowest layer at about 30 m above ground level. The second set (G2) is triply nested: a 36 km resolution grid is the same as that in G1, while a nested 12 km grid (88 by 88 grid points) includes a 4 km grid (163 by 199) covering most of California (fig. 1b). A total of 50 σ layers are used in G2, with the lowest layer at about 15 m above ground level. In all the experiments using the G1 grid configuration, the interaction between the 36 km and 12 km grids is two-way. However, in those experiments using the G2 grid configuration, the interaction between the 36 km and 12 km grids is one way, while that between the 12 km and 4 km grids is two way.

The model is initialized at 1200 UTC 2 February 1998 and all simulations are carried out for 36 hours. The gridded data used to initialize the model are obtained by performing a successive-scan objective analysis on conventional surface and rawinsonde observations. The first-guess fields used in obtaining the data are the gridded global analyses of wind, temperature, geopotential, and relative humidity at the mandatory levels from the National Centers for Environmental Prediction (NCEP).

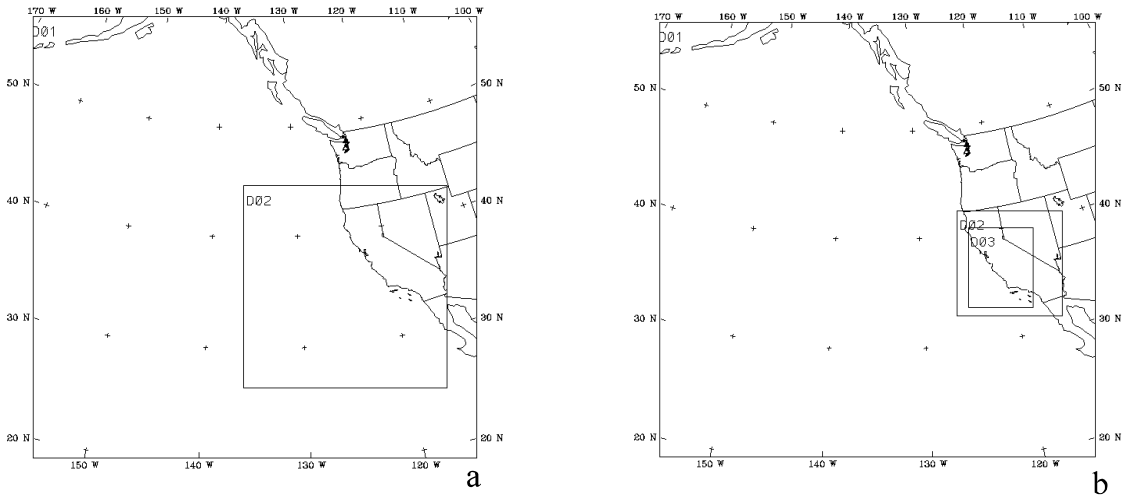

Figure 1. Two sets of nested grids are used in this study: (a) G1: a 36 km resolution grid (121 by 121 grid points) containing a nested 12 km grid (166 by 166 grid points); (b) G2: a 36 km resolution grid same as that in G1 containing a nested 12 km grid (88 by 88 grid points) which includes a 4 km grid (163 by 199).

The P-3 aircraft data are assimilated into the model during the model integration through "nudging", a continuous and dynamic data assimilation method (Stauffer and Seaman, 1994).

b. Assimilation method for P-3 aircraft data

In the nudging method, a forcing function is added to one or more of the prognostic equations of an explicit dynamic model, such that the model state is gradually "nudged" toward the observations based on the difference between the two (see, e.g., Anthes, 1974). In the observation nudging method, a nudging term appears in the prognostic equation for variable α as follows:

$$\frac{\partial \alpha}{\partial t} = F(\alpha, \vec{x}, t) + \varphi_\alpha \frac{\sum_{t=1}^{N} W^2(\vec{x}, t)\, \gamma_t\, (\alpha_o - \overline{\alpha})}{\sum_{t=1}^{N} W^2(\vec{x}, t)} \quad ,$$

where F = all of the model's physical forcing terms, φ_α = the nudging constant for the predictive variable α, W = the four-dimensional weighting function, α_o = the observations of α, $\overline{\alpha}$ = the model-predicted α interpolated to location of α_o, γ = the factor for observation quality control, and N = the number of observations within a four-dimensional region of influence around a given grid point.

c. Experiment design

To examine the impact of the P-3 aircraft data on the forecast of the cyclone system, two sets of experiments are performed with grid configurations of G1 and G2, respectively. For G1, data assimilation is carried out on the 12 km grid, while for G2 it is on the 36 km grid. In the in situ data set, there are a total of 14 dropsonde profiles of temperature, moisture, and wind between the surface and about 500 mb, taken from1030 to1330 UTC 2 February; there are an additional 14 soundings of temperature and wind derived from P-3 ascents and descents between 1000 mb and 850 mb, and from 1330 to1830 UTC 2 February. Experiments with and without data assimilation are carried out to examine the difference. The planetary boundary layer (PBL) scheme (Hong and Pan, 1996) of the NCEP medium-range forecast model (MRF) and a mixed-phase explicit moisture scheme (Reisner et al., 1998) are used in all the experiments on all the grids. The Anthes-Kuo (Anthes, 1977), Kain-Fritsch (Kain and Fritsch, 1993), Grell (Grell,1993) and the Betts-Miller (Betts and Miller, 1986) schemes are used in this study to investigate the sensitivity of the data impact to different convective parameterization schemes. Details about the experiments are summarized in tables 1 and 2.

4. RESULTS OF NUMERICAL EXPERIMENTS

a. Data impact

The experiment using the Anthes-Kuo scheme (AK) yields a cyclone system whose sea level pressure pattern and low center motion are most consistent with the NCEP analyses (not shown). The experiment using AK produces a cyclone that moves northeast during the period of simulation, while

those using the other schemes move toward the east after 0000 UTC 3 February. Thus, in this section, only the experiments using AK will be presented to show the impact of in situ observations on downstream forecasts.

The impact of the CALJET data assimilation can be seen clearly in the low-level wind field. Figure 2 compares the 925 mb wind speed at 1800 UTC 2 February (6 h after the initial time) of the experiment without the data assimilation (CNTLAK in table 1, fig. 2a) to the experiment with data assimilation (OBSAK in table 1, fig. 2b). All the P-3 data available on 2 February has been assimilated into the model by this time. Note that in OBSAK, the area of strong winds in the warm sector is broader than in CNTLAK and, as a result, there is a stronger shear zone to the north of the LLJ in OBSAK. The change of wind speed with the data assimilation at 925 mb is as great as 13.4 $m\ s^{-1}$; the wind direction fields, however (not shown), are not significantly different. The broader area of strong winds indicates that the position of the LLJ in the model output is different than that shown by the data. Further careful comparison of aircraft and satellite data with the pattern of low-level winds in the model output shows that the front and the LLJ are too far east in the experiment without the data assimilation, yet the assimilation does not alter the position of the front.

There are no significant differences between the wind speeds in OBSAK and CNTLAK along the coast of northern California at 1800 UTC 2 February. As the frontal system approaches the coast, however, wind speed differences along the coast begin to appear, although the differences are not as much as those seen in figure 2. Between 1800 UTC 2 February and 0000 UTC 3 February, the winds in the lowest 1300 m in northern California are generally faster in CNTLAK than in OBSAK. After 0000 UTC 3 February, however, the difference pattern changes. Between 0100 - 1000 UTC 3 February, the mean low-level wind in northern California becomes faster in OBSAK than in CNTLAK. The temporal change of the wind difference in northern California suggests that the wind and mass fields are undergoing adjustment, which is caused by the modification of the model state in the upstream area where observations are assimilated.

Differences in precipitation are also evident. Figure 3a shows the pattern of 6 h accumulated precipitation (in mm) ending at 0600 UTC 3 February for CNTLAK. By this time, the main rain band ahead of the cold front has come onshore in central and northern California, with MM5 producing as much as 99 mm of rain in 6 h along the California coast south of Monterey Bay. While the

Table 1. Summary of experiments with G1 grid configuration

Name of Experiment	Convective Parameterization scheme	Assimilation of P-3 data
CNTLAK	Anthes-Kuo (all grids)	None
OBSAK	Anthes-Kuo (all grids)	On 12 km grid
CNTLKF	Kain-Fritsch (all grids)	None
OBSKF	Kain-Fritsch (all grids)	On 12 km grid
CNTLGR	Grell (all grids)	None
OBSGR	Grell (all grids)	On 12 km grid
CNTLBM	Betts-Miller (all grids)	None
OBSBM	Betts-Miller (all grids)	On 12 km grid

Table 2. Summary of experiments with G2 grid configuration

Name of Experiment	Convective Parameterization scheme	Assimilation of P-3 data
CNTLG2	Anthes-Kuo on 36 km grid Kain-Fritsch on 12 km grid None on 4 km grid	None
OBSG2	Anthes-Kuo on 36 km grid Kain-Fritsch on 12 km grid None on 4 km grid	On 36 km grid

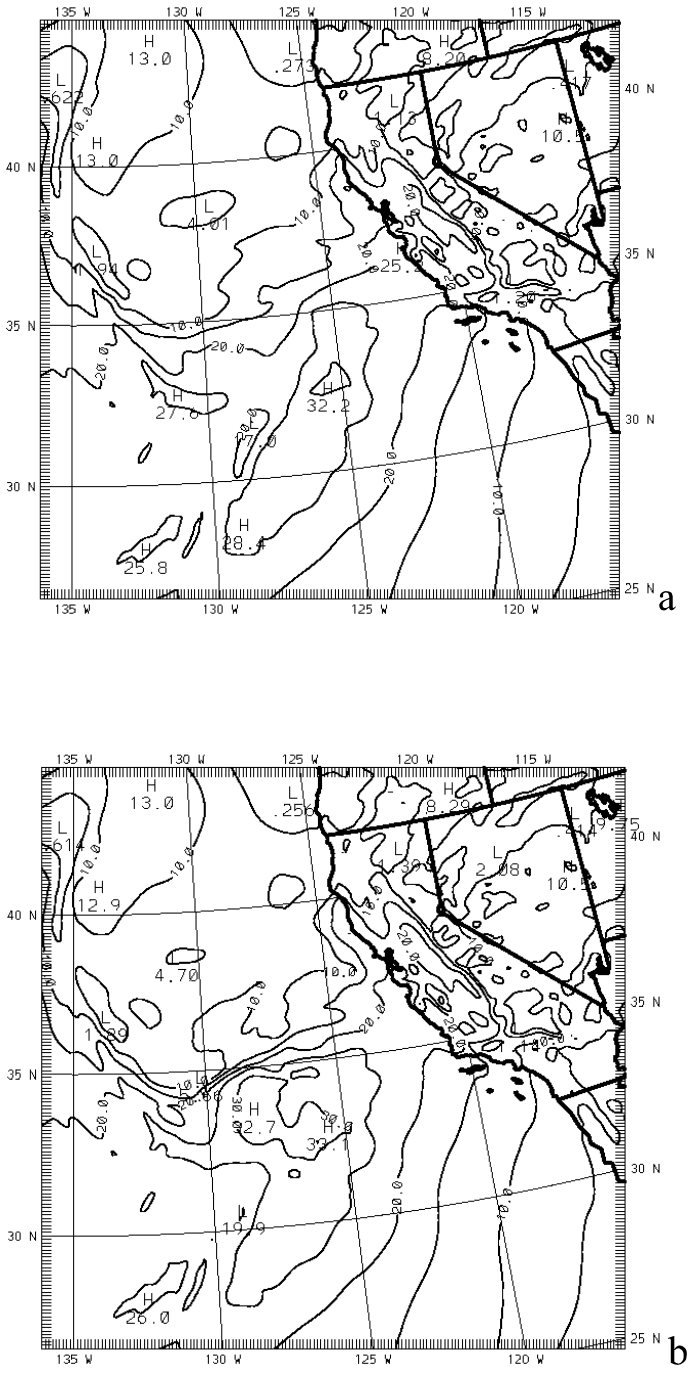

Figure 2. Wind speeds (m/s) in (a) CNTLAK and (b) OBSAK and verifying at 1800 UTC 2 February 1998.

precipitation pattern in OBSAK appears similar (not shown), there are some mesoscale differences, as seen in figure 3b. The differences are especially apparent northeast of the San Francisco Bay area, where there is as much as 33 mm more precipitation in CNTLAK, and along the coast south of Monterey Bay, where the difference is as much as 37 mm more in CNTLAK. There are two areas in which OBSAK has more precipitation than CNTLAK (24 and 34 mm), indicating that the areas of local maximum rainfall have been apparently moved by the addition of the experimental data.

These differences indicate that the assimilation of the CALJET data do have an apparent impact on the precipitation forecasting in California. To determine whether the impact of the in situ data leads to a better forecast, bias and threat scores for precipitation are calculated. Table 3 shows

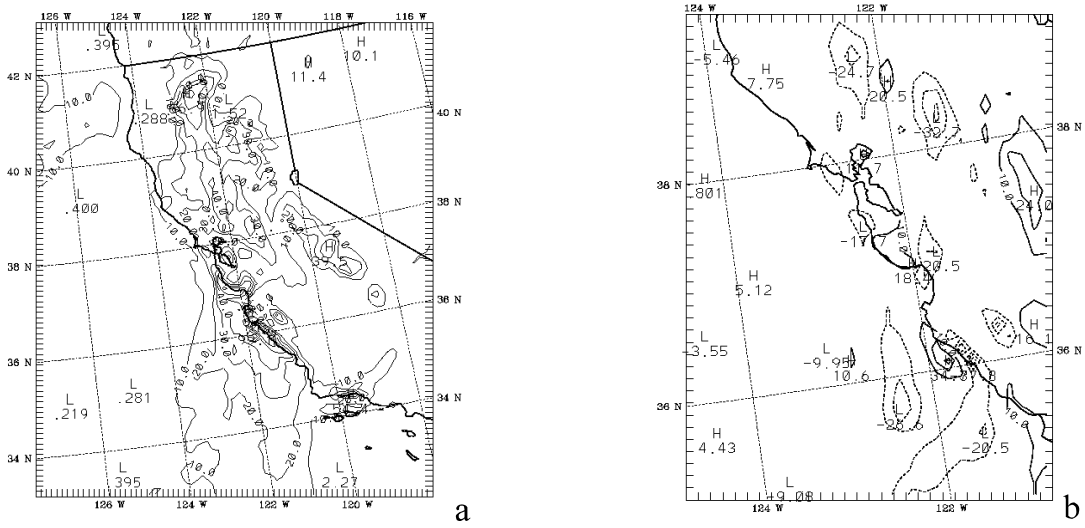

Figure 3. (a) the pattern of 6 h accumulated precipitation (in mm) ending 0600 UTC 3 February 1998 for CNTLAK, and (b) the difference of 6 h accumulated precipitation (in mm) ending at 0600 UTC 3 February 1998 between OBSAK and CNTLAK.

the bias and threat scores (Wilks, 1995) for hourly accumulated precipitation for both CNTLAK and OBSAK averaged from 0000 UTC to 1200 UTC 3 February. The data used for this verification are the hourly rain gauge data from the National Climatic Data Center (NCDC). Since most of the differences in precipitation between CNTLAK and OBSAK occur in the area of figure 3b, only data located within this area are included in the calculation of bias and threat scores. Also, the bias and threat scores are both calculated using a threshold of 0.001 mm. This means that the statistics take into account only whether or not there is precipitation. Given the fact that 28 observations are

available for verification in this area, the difference between the bias and threat scores for OBSAK and CNTLAK can be considered as statistically small.

Table 3. Bias and threat scores for precipitation averaged over the 12 h time period of 0000 UTC to 1200 UTC 3 February at the 0.001 mm threshold (statistics are calculated only over the area shown in fig. 3b).

Experiment	Bias Score	Threat score
CNTLAK	1.23	0.567
OBSAK	1.15	0.530

The results from CNTLG2 and OBSG2 (see table 2 for configurations) are verified as well. Figure 4a shows that root-mean-square (rms) wind direction errors at 1.0 km above the mean sea level indicate no significant difference between the control and data assimilation experiments. The data used in the verification were obtained from 10 ETL 915 MHZ costal wind profilers (for locations, see Ralph et al., 1999). Errors in wind speed errors (fig. 4b) are slightly (~1.0-1.5 m/s) improved between 2000 UTC 2 February and 0200 UTC 3 February. However, the difference plots suggest that this improvement could be incidental and due to the model's adjusting to the assimilation. Since the model forecasted LLJ reaches the coast between 0000 UTC and 0600 UTC 3 February, this is the time of most interest as far as improving the forecast is concerned. However, since only a slight improvement (less than1 m/s) in the rms wind speed errors can be seen, the data impact is insignificant. Figures 4c and 4d depict the threat and bias scores from verification against the NCDC's hourly rain gauge data. These skill scores are computed over all stations in California using 12 h accumulated precipitation. While the bias scores (fig. 4c) show a degradation in the precipitation forecast with the addition of the data assimilation, the threat scores (fig. 4d) show some improvement. This indicates that the better forecast shown by the threat scores is achieved by overpredicting the precipitation in the data assimilation experiment. Nevertheless, the data impact, if any, is not great.

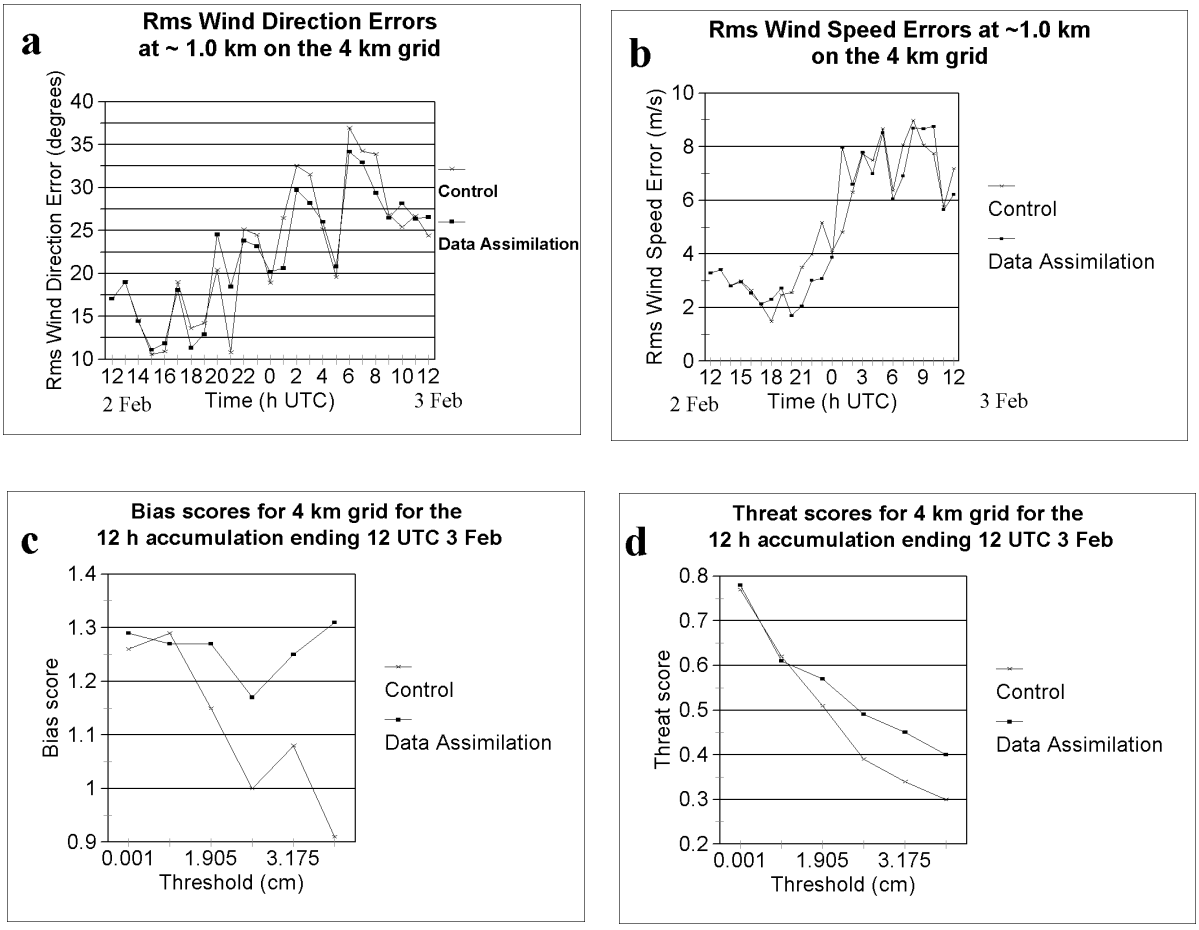

Figure 4. (a) and (b) are the rms wind direction and wind speed errors at 1.0 km above mean sea level; (c) and (d) depict the threat and bias scores from the verification against NCDC's hourly rain gauge data; these skill scores are computed over all stations in California using 12 h accumulated precipitation.

b. Sensitivity of data impact to convective parameterization schemes

As previously mentioned, the evolution of the cyclone system in this case is sensitive to the convective paramaterization scheme used. The simulations using the Kain-Fritsch (KF), Grell (GR), and Betts-Miller (BM) schemes all show a similar deviation in the cyclone's evolution from the NCEP analyses. Therefore, the discussion of the sensitivity of data impact to convective parameterization schemes will focus on a comparison of numerical simulations using only one of

these three schemes, KF, with simulations using AK.

Figure 5 shows the sea level pressure patterns from CNTLKF (fig. 5a) and CNTLAK (fig. 5b) verifying at 1200 UTC 3 February 1998. Neither simulation includes data assimilation. The differences between the two simulations are clearly evident. CNTLAK brings the cyclone farther north (by about 400 km), closer to that being analyzed (dots in fig. 5). The position of the cold front in CNTLAK in southern California is much closer to the observed position than in CNTLKF. Also note that the orientation of the cyclone is different and that the part of the cold front in southern California is slightly faster in CNTLKF (as indicated by the trough position). The sea level pressure correlation between the simulations and NCEP's analyses (table 4) confirms that CNTLAK is in closer agreement to what is analyzed than CNTLKF. It is also seen in table 4 that the differences between the two become significant after 12 h into the simulation.

When the P-3 data are assimilated in the model (i.e., OBSKF and OBSAK), the sea level pressure correlation between the simulations and NCEP's analyses are similar to that shown in table 4. What is interesting, however, is that the difference in the precipitation forecasts at the coast is not as much as that shown in the sea level pressure fields. Table 5 shows the bias and threat scores for the simulations with (OBSKF) and without (CNTLKF) data assimilation for hourly accumulated precipitation averaged from 0000 UTC to 1200 UTC 3 February. For the number of observations used in the verification, the differences between the scores with and without data assimilation in table 5 and those in table 3 are statistically small. Therefore, the sensitivity of data impact on the precipitation forecasts at the coast to convective parameterization schemes is minimal. However, the position of the cyclone (see table 4) is sensitive to the choice of convective parameterization schemes.

Table 4. Sea level pressure correlation between model simulation and NCEP's analysis over a box surrounding the low-pressure center of the analysis.

Time (Day/UTC)	Hours into Simulation	CNTLAK	CNTLKF
3/0000	12	0.882	0.923
3/1200	24	0.914	0.731
4/0000	36	0.879	0.463

Table 5. Same as table 3, but for simulations using KF.

Experiment	Bias Score	Threat score
CNTLKF	1.49	0.627
OBSKF	1.39	0.606

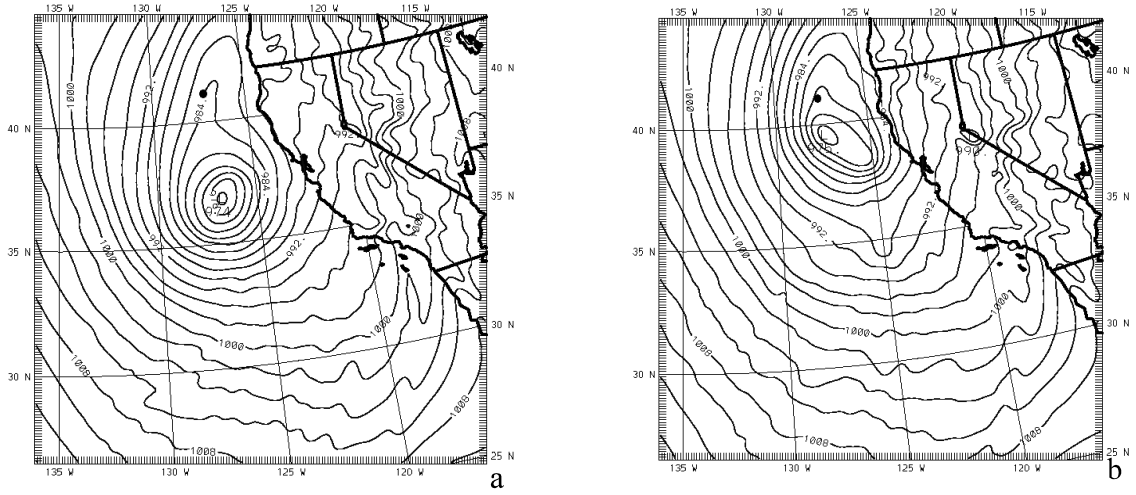

Figure 5. The sea level pressure patterns (in mb) from CNTLKF (a) and CNTLAK (b) verifying at 1200 UTC 3 February. Dots indicate NCEP's analyzed low center.

5. ADJOINT SENSITIVITY AND TRAJECTORY ANALYSES

a. Adjoint sensitivity analysis

Because only the adjoint of the tangent linear version of a simplified physics version of MM5

is available, a simulation from the same initial condition is first produced with the simplified-physics version of MM5. It is found that the differences in the LLJ between the simplified version and the full physics version are small before the onset of heavy rainfall as the cold front moves onshore. It is expected, therefore, that the adjoint will be able to approximate the sensitivity of the output of the complicated physics version of MM5 to perturbations in the initial conditions. The simplified-physics version of MM5 uses an explicit scheme that simply removes supersaturation as precipitation and adds the latent heat to the thermodynamic equation (Zou and Kuo, 1996). A bulk scheme is used for PBL processes. Since the adjoint is not capable of handling two-way, interacting, nested grids, the sensitivity analysis is performed only on the 36 km grid.

The sensitivity of the surface wind over the northern California coast with respect to perturbations in the initial state is analyzed using the adjoint model. Specifically, the u component of the wind speed of a grid point near Bodega Bay, at the lowest σ level at 0000 UTC 3 February, is defined as the cost function; the gradient of this cost function with respect to the model state is taken as the initial input of the adjoint model. The sensitivity of the u (approximately onshore) component is examined rather than that of the v (approximately alongshore) component because all the experiments conducted in this study have indicated that the heavy rainfall in northern and central California associated with the storm is much more sensitive to the u component. Wind speed could be another choice of the cost function. Yet wind speed has ambiguity of wind direction, which is crucial in causing heavy rainfall in mountainous northern and central California.

Figure 6 shows the sensitivity of the aforementioned cost function with respect to u and v components of the wind 6 h before, at σ = 0.988 (fig. 6a) and σ = 0.350 (fig. 6b). While the maximum and minimum axes tilt upstream with height, the horizontal maximum magnitude of the sensitivity varies with height (between 0.24 and 0.78, with the larger ones being at the lower levels). It is interesting to note that in figure 6 the area with the most sensitivity at the lower level does not correspond with the area where the LLJ was observed by the dropsondes from P-3 aircraft during CALJET. Although the area with the most sensitivity at the upper level coincides with the area where the P-3 observations were made, it is at the higher level that the dropsondes were released. This explains why the P-3 data have minimal impact on the prediction 6 h later of the wind and consequential precipitation along the coast.

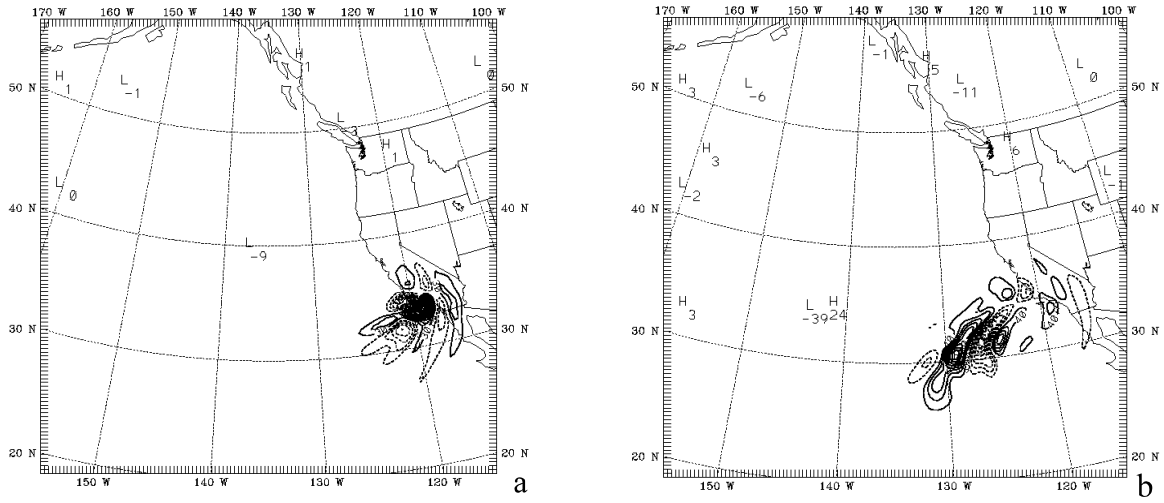

Figure 6. The sensitivity of the cost function mentioned in the text with respect to the u component of the wind 6 h before at $\sigma = 0.988$ (a) and $\sigma = 0.350$ (b). All the contours are scaled by 10^3 with the interval being 30 in (a) and 40 in (b); negative values are dashed. The extreme values are -0.26 and 0.35 in (a), and -0.335 and 0.359 in (b).

b. Trajectory analysis

Another fundamental approach to understanding the impact of the P-3 aircraft data on the prediction of the LLJ and coastal wind and precipitation, as shown by the above results of numerical experiments and the adjoint sensitivity analysis, is to diagnose the trajectory movement of air parcels. From the Lagrangian point of view, observations affect the evolution of the state of an air parcel only when they are taken and assimilated into the model upstream, along the parcel trajectory. Figure 7a shows the forward trajectories of the air parcels at the core of the LLJ at 900 m above the sea surface. The air trajectories are released at 1800 UTC 2 February when the core of the LLJ is modified by the assimilation of the P-3 aircraft data. It is seen that these trajectories move aloft afterward, along the so-called warm conveyor belt. Figure 7b depicts the backward trajectories released from the core of the LLJ that impinges the coast at 0000 UTC February. It is seen that the core at the coast is made of air parcels originating from a different location than these of the core at 1800 UTC 2 February. These trajectory diagnoses show why the impact of the P-3 aircraft data on the simulation of the LLJ is minimal at a later time, when the LLJ impinges on the coast. At the core's level, air parcels accelerate as they move from the warm sector toward the LLJ region. When they enter the LLJ

region, the parcels start to move aloft. Hence, processes well within the warm sector affect the properties of the coastal LLJ region, while the properties of the LLJ region offshore affect the properties of the coastal air at 3 to 5 km. Although it has been hypothesized that both of these levels play important roles in affecting coastal topographic precipitation, the results from this case

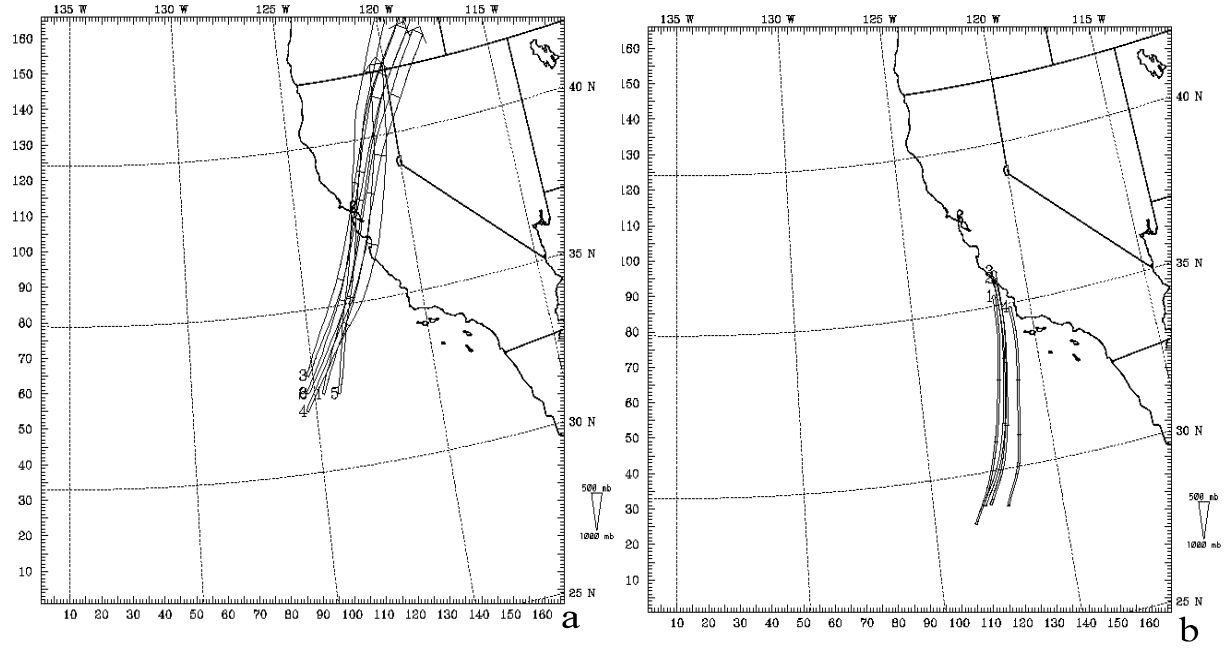

Figure 7. (a) The forward trajectories of the air parcels at the core of the LLJ at level 900 m above the sea surface, released at 1800 UTC 2 February when the core of the LLJ is modified by the assimilation of the P-3 aircraft data; (b) the backward trajectories released from the core of the LLJ that impinges on the coast at 0000 UTC February; the height of the trajectories is shown by the width of the ribbon.

study suggest that changes to the air aloft have minimal impact on coastal precipitation.

6. SUMMARY AND DISCUSSION

In this study, numerical experiments are carried out to assess the impact of CALJET P-3 aircraft data on the forecast of winds and precipitation over the California coast associated with a landfalling storm. Since only one model is used in a single case study, the results should be viewed

as limited.

In the experiments, the nudging method is used for the assimilation of dropsonde data (between the surface and 500 mb) and flight-level soundings (between 1000 and 850 mb) observed over an approximately 6 h period. The low-level winds in the model at 6 h into the simulation are changed significantly by the data assimilation, but the model forecasted movement of the cyclone, which is different from observations, is not altered.

The major finding is that the P-3 data have a minimal impact on the 12 to 24 h coastal wind and precipitation forecasts. This is reflected by the fact that the threat and bias scores for hourly precipitation are changed only slightly by the assimilation of the data. This minimal impact does not appear to change with different convective parameterization schemes, although the simulated cyclone position 12 to 36 h into the forecast is affected by the choice of schemes. One possible explanation for the minimal data impact is that in this case, the errors in the coastal wind and precipitation forecasts are due mainly to errors in the position of the cyclone and front; the P-3 data are not sufficient to correct them (more details on this aspect will be discussed in a later report).

The adjoint sensitivity analysis suggests another possible explanation for the minimal data impact. The sensitivity results indicate that the P-3 observations were not taken in the area where the forecasted evolution of the surface wind associated with the LLJ is most sensitive to the perturbations of the model state. Further trajectory analyses support this explanation. It is suggested that in order for observations to affect the evolution of the state of an air parcel, they should be taken and assimilated into the model upstream along the parcel's trajectory.

The minimal impact of the P-3 data may also have been caused by a lack of effectiveness in the data assimilation method. However, to verify whether this is the case, more research is required. In future research, at least one different data assimilation method, such as the 3D/4D variational method, should be used and compared with the method used in this study.

It is worth noting that these same data, which do not significantly affect the model-based quantitative precipitation forecast (QPF) in this case, nonetheless allowed human forecasters to issue a flash flood warning (Ralph et al., 1999) based on a conceptual model. This does not contradict the result of the minimal impact on the model QPF because it is generally acknowledged that a strong LLJ offshore is associated with an intense frontal system, and the latter often brings strong winds and heavy precipitation onshore when it makes landfall. During the field experiment, the P-3

observations provided quantitative observations of the strength and height of the LLJ offshore, which then were used in "rules of thumb" developed by forecasters, assuming the observed offshore strength and height of the LLJ persisted until landfall. Such information was not available from any other observational system.

Two related aspects of these results are worth further discussion. First, while the cyclone evolutions differ greatly in the numerical experiments when different convective parameterization schemes are used, the forecasted coastal precipitation patterns do not. This suggests that, as depicted by the model for this case, precipitation patterns along the California coast appear to be indifferent to discrepancies in the position of the cyclone center. Thus, the heavy coastal precipitation in the numerical experiments is tied to other aspects of the storm, such as the moist south-southwesterly flow interacting with the coastal topography.

Second, the influence of in situ data diminishes by the time the LLJ reached the coast. This suggests that the model forecasted LLJ, which is an important factor for producing precipitation in the coastal region, may have undergone a change that is not simply due to advection. This is consistent with the explanation, based on both the adjoint and trajectory analyses, on why the impact of the in situ data is minimal.

7. REFERENCES

Anthes, R.A., 1974. Data assimilation and initialization of hurricane prediction models. *J. Atmos. Sci*., **31**: 702-719.

Anthes, R. A., 1977. A cumulus parameterization scheme for a one-dimensional cloud model. *Mon. Wea. Rev*., **105**: 270-286.

Betts, A. K. and M. J. Miller, 1986. A new convective adjustment scheme. Part II: Single column test using GATE wave, BOMEX, ATEX and Artic air-mass data sets. *Quart. J. Roy. Meteor. Soc*., **112**: 677-692.

Grell , G. A., 1993. Prognostic evaluation of assumptions used by cumulus parameterizations. *Mon. Wea. Rev.*, **120**: 764-787.

Grell, G. A., J. Dudhia and D. R. Stauffer, 1994. A description of the fifth-generation Penn State/NCAR mesoscale model (MM5). NCAR Tech. Note, TN-398+STR, National Center for Atmospheric Research, Boulder, CO, 80307, 122 pp.

Hong, S. -Y., and H. -L. Pan, 1996. Nonlocal boundary layer vertical diffusion in a medium-range forecast model. *Mon. Wea. Rev.*, **124**: 2322-2339.

Kain, J. S., and J. M. Fritsch, 1993. Convective parameterization for mesoscale models: The Kain-Fritsch scheme. In: *The Representation of Cumulus Convection in Numerical Models, Meteor. Monogr.* No. 46, Amer. Meteor. Soc., 165-170.

Ralph, F. M., P. O. G. Persson, D. Reynolds, W. Nuss, D. Miller, J. Schmidt, D. Jorgenson, J. Wilczak, P. Neiman, J.-W. Bao, D. Kingsmill, Z. Toth, C. Veldon, A. White, C. King, and J. Wurman, 1999. The California Land-Falling Jets Experiments (CALJET): Objectives and design of a coastal atmosphere-ocean observing system developed during a strong El Niño, *3rd Symposium on Integrated Observing Systems*, Dallas, TX, 10-15 Jan 1999, 78-81.

Reisner, J., R. M. Rasmussen, and R. T. Bruintjes, 1998. Explicit forecasting of supercooled liquid water in winter storms using the MM5 mesoscale model. *Quart. J. Roy. Metero. Soc.*, **124B**: 1071-1107.

Stauffer, D. R. and N. L. Seaman, 1994. Multiscale four dimensional data assimilation. *J. Appl. Meteor.*, **33**: 416-434.

Wilks, D. S., 1995. *Statistical Methods in the Atmospheric Sciences.* Academic Press, San Diego, CA, 467 pp.

X. Zou, and Y.-H. Kuo, 1996. Rainfall assimilation through an optimal control of initial and boundary conditions in a limited-area mesoscale model. *Mon. Wea. Rev.*, **124**: 2859-2882.